Palaeontologia Electronica
palaeo-electronica.org

Trilobite moulting behaviour variability had little association with body proportions

Harriet B. Drage

ABSTRACT

Trilobite moult assemblages preserved in the fossil record show high variability in moulting behaviour and their resulting moult configurations. The reasons for this variability, and the impacts it might have had on trilobite evolutionary trajectories, are unknown and have rarely been investigated quantitatively. A large dataset of trilobite moult traditional morphometric measurements is presented and statistically analysed for associations between moulting behaviour and morphometry. Results indicate little significant statistical association between the two; only between moulting behaviour (usually generalised moult configuration) and the variances and means of thoracic tergite number, thoracic length, and pygidial width. Anterior cranidial width, cranidial length, cephalothoracic joint width, thoracic width, pygidial length, and total body length all have non-significant associations with moulting behaviour. Moult specimens showing inversion of the librigenae generally have more thoracic tergites, a correspondingly longer thorax, and a narrower pygidium. Thoracic tergite count and pygidium measurements may have multimodal distributions. Principal Components Analyses and Non-Metric Multidimensional Scaling analyses suggest that moulting behaviour groups show minor differences in the extent of their morphometric variation, but little difference in the region of morphospace they occupy. This may indicate that trilobite species using Salter's mode of moulting had more constrained morphologies, potentially related to facial suture fusion in some groups. Overall, these results do not suggest a strong association between moulting behaviour variation and morphometry in trilobites, leaving open for further study the mystery of why trilobites were so variable in their moulting, and whether this contributed to their long evolutionary reign or ultimate extinction.

Harriet B. Drage. Institute of Earth Sciences, University of Lausanne, Géopolis, 1015 Lausanne, Switzerland. harriet.drage@unil.ch

Keywords: disparity; moulting; morphometry; morphospace; multimodal distribution; trilobite

Final citation: Drage, Harriet B. 2024. Trilobite moulting behaviour variability had little association with body proportions. Palaeontologia Electronica, 27(1):a9.
https://doi.org/10.26879/1265
palaeo-electronica.org/content/2024/5123-trilobite-moulting-morphometry

Submission: 3 January 2023. Acceptance: 12 January 2024.

INTRODUCTION

Exoskeleton moulting is a key recurrent event in the life histories of all euarthropods. The exoskeleton protects individuals from predation and parasitism (Ewer, 2005), but is naturally restrictive so must be periodically moulted for significant growth and developmental changes to occur. This moulting is energetically expensive and leaves the individual periodically more vulnerable to predation during exuviation (exiting of the old exoskeleton) and during reinforcement of the new exoskeleton (Vevea and Hall, 1984). The behaviours and mechanisms involved in moulting are therefore inherently linked to euarthropod morphology, development, ecology, and broad-scale evolution (Brandt, 2002; Daley and Drage, 2016). The fossil record of euarthropod moulting is extensive (see Daley and Drage, 2016), allowing exploration of the interactions between moulting behaviour and these key biological facets.

Trilobites have a rich fossil record of moults with which to explore the impact of moulting behaviours on their evolution (e.g., Henningsmoen, 1975; McNamara and Rudkin, 1984; Whittington, 1990; Brandt, 2002; Budil and Bruthansová, 2005; Drage, 2019a; Drage et al., 2019, 2023a; Corrales-García et al., 2020; Wang et al., 2021, 2023; Zong, 2020; Piccoli et al., 2021; Zong and Gong, 2022; see Daley and Drage, 2016, for a more exhaustive list), owing to their exoskeletons reinforced with calcite that have a high preservation potential (Teigler and Towe, 1975). Further, trilobites are unusual because they appear to show a greater range of moulting behaviours and preserved moulting configurations (the configuration of disarticulated sclerites preserved in the fossil record and reflecting moulting movements) than other euarthropod groups with apparently specialised moulting behaviours leading to recognisable configurations (Brandt, 2002; Daley and Drage, 2016; Drage, 2019a,b). Not only do trilobites show high interspecific variability in their moulting, but also seemingly extensive intraspecific variation, with different individuals of the same species preserving varied configurations (see Drage et al., 2018a). Trilobites are also one of the most successful groups of euarthropods based on their diversity of ecological niches, abundance, global distribution, and evolutionary timespan (Fortey and Whittington, 1989; Fortey and Owens, 1999; Webster, 2007).

Trilobites show the evolution of a variety of sophisticated sutures involved in moulting, for example, the cephalic sutures, which may exist solely to facilitate moulting through disarticulating the librigenae and producing an anterior exuvial gape (Stubblefield, 1959; Hughes, 2007; Hou et al., 2017; Du et al., 2019). The facial sutures were also secondarily lost in some groups (see Daley and Drage, 2016) or occasionally fused during development (Drage et al., 2018b; Esteve and Hughes, 2023). A variety of other cephalic sutures were used for moulting in some groups, such as an anterior marginal suture, rostral and hypostomal sutures, and ventral median sutures, as well as important use of the cephalothoracic joint for moulting (Henningsmoen, 1975; Fortey, 2001; Budil and Bruthansova, 2005; Drage, 2019b). Consequently, trilobites display several modes of moulting, which can be summarised into the following, distinguished by their relevant morphological features (see Table 1):

1 use of the cephalic exuvial sutures (various combinations of facial, rostral, and hypostomal sutures depending on morphology), termed the Sutural Gape mode of moulting
2 use of the cephalothoracic joint for moulting, termed Salter's mode of moulting
3 use of the marginal suture along the anterior cephalic margin (Henningsmoen, 1975; Drage, 2019b).

In concert with the individual movements of trilobites, these produce an array of moult configurations that are found preserved in the fossil record (Figure 1). Drage et al. (2018a) described and named a number of these pertaining to the Sutural Gape and Salter's modes of moulting using an exceptionally preserved, diverse sample of *Estaingia bilobata* Pocock, 1964.

Several early works emphasised the potential important impacts of trilobite moulting behaviour variability on their evolutionary trajectories (e.g., Henningsmoen, 1975; Whittington, 1990; Budil and Bruthansova, 2005) and the potential impact of this behaviour on their extensive success and ultimate decline (Brandt, 2002). Recent studies have described moulting in specific trilobite groups, such as Zong (2020) on moults of *Ovalocephalus tetrasulcatus* Kielan, 1960, arranged end-to-end, syn-

TABLE 1. Moulting behaviour terminology used throughout this work. Details of the specific moult configurations described for trilobites can be found in Drage et al. (2018a). For examples see Figure 1.

Modes of moulting used in this study	Sutural Gape mode of moulting	Mode of moulting that involves only opening of the cephalic sutures, which may comprise the facial, rostral, and/or hypostomal sutures.
	Salter's mode of moulting	Mode of moulting that involves only opening of the cephalothoracic joint during moulting, causing disarticulation of the cephalon.
	Hybrid mode of moulting	Mode of moulting combining both the Sutural Gape and Salter's modes, with both cephalic sutures and the cephalothoracic joint opening during moulting.
Generalised moult configurations used in this study	Cephalic sutures configuration	Preserved moult configurations that have variously opened cephalic sutures, and so have related cephalic sclerites disarticulated from the body (librigenae, rostral plate, and/or hypostome). This includes moults in Harrington's, Nutcracker, and Axial Shield configurations (of Drage et al., 2018a).
	Cephalic sutures + inversion configuration	As above, but with some of the disarticulated cephalic sclerites, usually librigenae, either horizontally or vertically flipped, as in the Somersault and McNamara's configurations respectively (Drage et al., 2018a).
	Salter's configuration	Moult configuration with the entire cephalon disarticulated at the cephalothoracic joint, and horizontally inverted compared to the remaining thoracopygon (Drage et al., 2018a).
	Zombie configuration	Moult configuration with the entire cephalon disarticulated at the cephalothoracic joint, and displaced from the remaining thoracopygon (Drage, 2019b).
	Henningsmoen's configuration	Moult configuration resulting from the hybrid mode of moulting, with the cephalon disarticulated at the cephalothoracic joint, but also the librigenae, rostral plate, and/or hypostome disarticulated (Drage et al., 2018a).

chronised moulting behaviour of several oryctocephalid species preserving diverse moulting configurations by Corrales-García et al. (2020), and ontogenetic moulting sequence trends in *Arthricocephalites xinzhaiheensis* Chen and Lin in Lu et al., 1974, by Wang et al. (2021). Other studies, notably Esteve et al. (2021), have investigated the variety of facial suture morphology, and the interaction between these moulting structures and trilobite ecology, with Esteve et al. (2021) suggesting that the movement of facial sutures to a dorsal position facilitated both stress reduction on the cephalon and variability in moulting behaviour. These studies have further increased support for inter- and intraspecific variability in moulting across Trilobita and its links with other aspects of morphology and behaviour. Indeed, all descriptions of the fossil record of moulting serve to further draw attention to and increase our understanding of this crucial behaviour in Euarthropoda (e.g., Daley and Drage, 2016; Yang et al., 2019; Mángano et al., 2020; Drage et al., 2023b; Moysiuk and Caron, 2023; Olempska et al., 2023). Drage (2019a) presented the first broad-scale study quantifying the extent of inter- and intraspecific variability in trilobite moulting, also exploring potential trends in moulting with taxonomic assignment and geological history. However, still little is known about why this moulting variability existed, the impacts it may have had on the evolutionary history of the group, and how moulting interacted with morphology.

This study uses the large dataset of trilobite moulting variability presented by Drage (2019a) and corresponding moult morphometric (comparative body proportion) measurements to test for an association between moulting behaviour and morphology. Body proportions may have impacted moulting behaviours, for example, differences in cephalic proportions might have changed exuvial gape sizes, making different disarticulations for moulting risky for the individual. Conversely, moulting may have imposed constraints on morphological evolution because certain disarticulations or exuvial gapes might have been incompatible with some morphologies.

MATERIAL AND METHODS

Data Collection

The dataset analysed here consists of descriptions of moulting configurations for 617 individuals of 132 trilobite genera and 238 species, which was originally presented by Drage (2019a). See the methodology described in Drage (2019a) for further details of specimen choice, location, and recording. Most specimens in the dataset were described and measured in person (by H.B. Drage). However, 46 out of 617 moults were

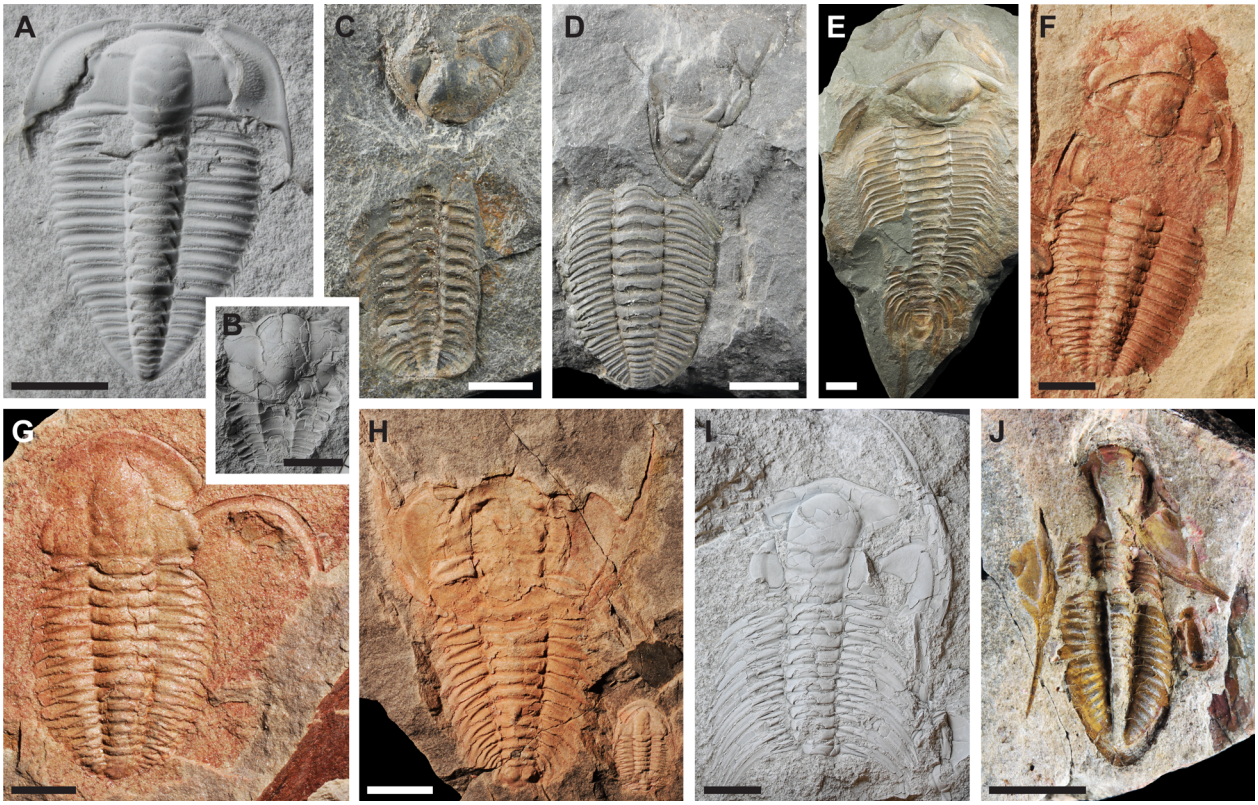

FIGURE 1. Trilobite generalised moult configurations featuring in the dataset presented here. A: *Olenus truncatus* Brünnich, 1781, PMU unnumbered specimen, cephalic sutures configuration group, B: *Ellipsocephalus* sp. Zenker, 1833, PMU 28642, Salter's configuration, C: *Trimerocephalus mastophthalmus* Richter, 1856, NHMUK I.5100, Salter's configuration, D: *Dalmanitina socialis* (Barrande, 1846), NHMUK 42341, Zombie configuration, E: *Paradoxides gracilis* Boeck, 1827, NHMUK 42440, Henningsmoen's configuration, F: *Estaingia bilobata* Pocock, 1964, SAM-P 46956, Henningsmoen's configuration, G: *Estaingia bilobata*, SAM-P 43767, cephalic sutures configuration group, H: *Redlichia takooensis* Lu, 1950, SAM-P 43593, Salter's configuration, I: *Accadoparadoxides pinus* Westergård, 1936, PMU 25995, cephalic sutures + inversion configuration group, J: *Phillipsia* sp. Portlock, 1843, NHMUK I.1092, cephalic sutures + inversion configuration group. Scale bars equal 5 mm for A, B, F, G, J; 10 mm for C–E, H, I.

included based on photographs from the descriptive literature (see Appendix); these were measured using Fiji (Schindelin et al., 2012). Most species are represented by a single specimen, though a considerable proportion of species (just under 40%) are represented by multiple individuals; the full counts for the dataset groupings at both a specimen and species level are given in Table 2. The decision to run analyses at the specimen rather than species level was made to maximise the data available, and because multiple specimen inclusion does not prevent hypothesis testing; whether moulting behaviour is linked to body proportions is testable regardless of species assignment.

Extensive literature searches were performed to confirm metadata regarding geological age range, taxonomic assignment, developmental stage, and species thoracic tergite count. However, some species descriptions are not readily available in the accessible literature; for example, information on complete thoracopygidia is not available for trilobite species originally described from isolated cephala (Whittington et al., 1997). Specimens that might have been of a juvenile developmental stage, based on thoracic tergite number and relative size, were removed from the dataset. This is because the inclusion of juveniles could bias results as immature individuals have been shown to moult differently to their adult counterparts in some species (e.g., Crônier and Fortey, 2006; Hughes et al., 2014; Drage et al., 2018b; Wang et al., 2021), and ontogenetic studies show that morphology can differ extensively between developmental stages (e.g., Park and Choi, 2011). It can be difficult to distinguish late-stage meraspides from holaspides, particularly if the tergite count is unavailable due to incomplete preservation,

TABLE 2. Number of specimens and unique species included in the dataset for each trilobite order, based on taxonomy of Adrain (2011). Count of specimens and unique species for each mode of moulting and generalised moult configuration (see Table 1 definitions) included in this study. '?' indicates some species-level taxonomic uncertainty. All raw specimen data available in the Appendix data file.

Order	# species	# specimens	Mode of moulting	# species	# specimens	Generalised moult configuration	# species	# specimens
Asaphida	?43	109	Sutural Gape	35	90	Cephalic sutures	34	88
			Salter's	10	11	Cephalic sutures + inversion	2	2
						Henningsmoen's	8	8
			Hybrid	8	8	Salter's	3	3
						Zombie	7	8
Aulacopleurida	7	37	Sutural Gape	5	35	Cephalic sutures	5	35
			Salter's	1	1	Cephalic sutures + inversion	0	0
						Henningsmoen's	1	1
			Hybrid	1	1	Salter's	0	0
						Zombie	1	1
Corynexochida	39	97	Sutural Gape	32	90	Cephalic sutures	31	89
			Salter's	3	3	Cephalic sutures + inversion	1	1
						Henningsmoen's	4	4
			Hybrid	4	4	Salter's	1	1
						Zombie	2	2
Lichida	3	4	Sutural Gape	2	2	Cephalic sutures	2	2
			Salter's	1	1	Cephalic sutures + inversion	0	0
						Henningsmoen's	1	1
			Hybrid	1	1	Salter's	1	1
						Zombie	0	0
Odontopleurida	11	23	Sutural Gape	8	20	Cephalic sutures	8	20
			Salter's	1	1	Cephalic sutures + inversion	0	0
						Henningsmoen's	2	2
			Hybrid	2	2	Salter's	1	1
						Zombie	0	0
Olenida	15	28	Sutural Gape	10	21	Cephalic sutures	10	21
			Salter's	1	1	Cephalic sutures + inversion	0	0
						Henningsmoen's	4	6
			Hybrid	4	6	Salter's	1	1
						Zombie	0	0

because many trilobite species are not known from enough juvenile specimens to describe their ontogenies, and some species also had variable numbers of tergites during functional adulthood (Hughes, 2007; Park and Choi, 2011; Esteve and Hughes, 2023). Thus, all species in the dataset have been checked in the descriptive literature to confirm adulthood, if possible, but a level of error resulting from accidental inclusion of late-stage meraspides remains plausible. In addition, specimens for which a moult assignment was uncertain were removed from the dataset, such as when there was too little associated material on the rock sample (only isolated thoracopygidia or cephala

TABLE 2 (continued).

Order	# species	# specimens	Mode of moulting	# species	# specimens	Generalised moult configuration	# species	# specimens
Phacopida	60	107	Sutural Gape	33	52	Cephalic sutures	28	46
			Salter's	31	46	Cephalic sutures + inversion	5	6
						Henningsmoen's	7	9
			Hybrid	7	9	Salter's	9	18
						Zombie	24	28
Proetida	9	13	Sutural Gape	7	11	Cephalic sutures	6	10
			Salter's	1	1	Cephalic sutures + inversion	1	1
						Henningsmoen's	1	1
			Hybrid	1	1	Salter's	0	0
						Zombie	1	1
?Ptychopariida	11	30	Sutural Gape	9	28	Cephalic sutures	11	28
			Salter's	0	0	Cephalic sutures + inversion	0	0
						Henningsmoen's	2	2
			Hybrid	2	2	Salter's	0	0
						Zombie	0	0
Redlichiida	?36	169	Sutural Gape	26	145	Cephalic sutures	32	130
			Salter's	4	6	Cephalic sutures + inversion	6	15
						Henningsmoen's	9	18
			Hybrid	9	18	Salter's	3	5
						Zombie	1	1

present) or material was highly fragmented (see moult designation criteria in Daley and Drage, 2016).

Linear measurements of key body dimensions were taken using digital callipers at the millimetre scale for each of the moult specimens, where possible given preservation, during the same period of data collection as for the data presented in Drage (2019a). These included (see Figure 2): anterior cranidial width (tr., between the anterior-most dorsal extension of the facial sutures in species with dorsal facial sutures, otherwise at a comparable location in species without dorsal facial sutures); cranidial axial length (sag.); cephalothoracic joint width (tr.); thoracic maximum width (tr., without pleural spines); thoracic axial length (sag.); pygidial maximum width (tr., without pygidial spines); pygidial axial length (sag.); and total axial body length (sag.). The thoracic tergite number was also recorded.

Each specimen was assigned both a mode of moulting (Sutural Gape, Salter's, or hybrid) and a generalised moult configuration (cephalic sutures, cephalic sutures + inversion, Salter's, Zombie, or Henningsmoen's configuration) – see full descriptions in Table 1. The 'cephalic sutures' configuration is defined as moults with the cephalic sutures open, without distinguishing between placement of the disarticulated sclerites in the preserved moult. The 'cephalic sutures + inversion' configuration is similar, but with horizontal or vertical inversion of the disarticulated librigenae. The 'hybrid' mode of moulting directly corresponds to Henningsmoen's configuration; this is a unique hybrid moult configuration displaying opening of both the cephalic sutures (Sutural Gape mode) and cephalothoracic joint (Salter's mode; Drage et al., 2018a). These generalised moult configurations were summarised from those named by Drage et al. (2018a). Due to the non-exceptional preservation of most specimens in the dataset, and the minimal contextual information associated with most accessioned museum species, it was not feasible to assign specific named moult configurations to most speci-

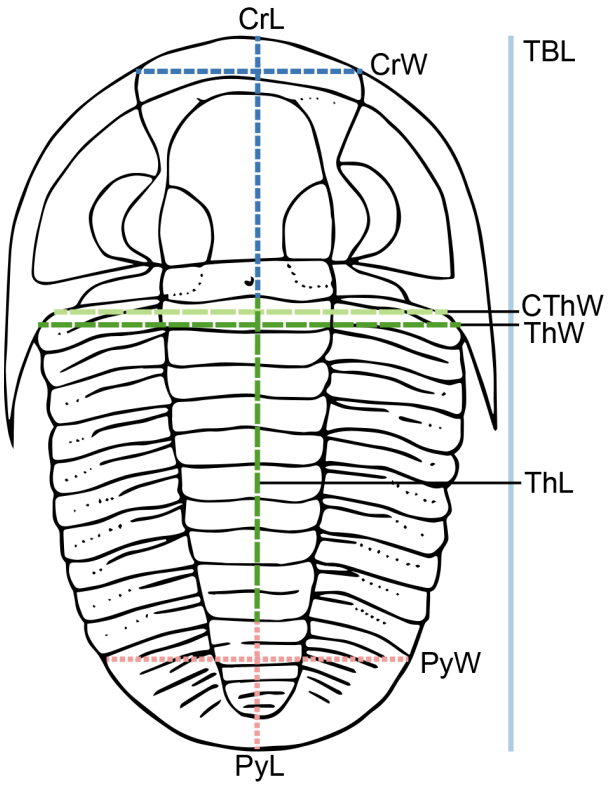

FIGURE 2. Illustration of measurements taken on trilobite specimens, where possible given specimen preservation, shown on simplified drawing of *Cryphoproetus*. CrW: cranidial width (tr.), CrL: cranidial axial length (sag.), CThW: cephalothoracic joint width (tr.), ThW: thoracic maximum width (tr.), ThL: thoracic axial length (sag.), PyW: pygidial maximum width (tr.), PyL: pygidial axial length (sag.), TBL: total axial body length (sag.).

mens. Accordingly, the cephalic sutures configuration combines the Nutcracker, Harrington's, and Axial Shield configurations of Drage et al. (2018a), and the cephalic sutures + inversion configuration combines the Somersault configuration and McNamara's configuration. Moult specimens with an open marginal suture were excluded from these analyses due to their small sample size.

Analysing the mode of moulting allows testing of the hypothesis 'trilobite body proportions did not significantly vary with their exuvial gape location (i.e., whether they moulted through use of dorsal facial sutures or through a gape at the cephalothoracic joint)'. This category does not test the importance of the movements used during moulting, and thereby minimises the impact of biostratinomic and other taphonomic biases. Analysing generalised moult configuration in addition to mode of moulting allows testing the hypothesis 'trilobite body proportions did not significantly vary with moulting behaviour (i.e., the entire suite of movements and behaviours employed to moult the old exoskeleton)', as the generalised moult configurations also include groupings that differ only in whether movements during moulting caused inversion of disarticulated sclerites, and not in the exuvial gape produced. Alterations to these generalised moult configuration groups from Drage et al. (2018a) were made, as discussed above, primarily to reduce the impact of taphonomic bias on moult fossil interpretation, as those configurations that could be most easily confused due to biostratinomy or decay have been grouped together (e.g., the cephalic sutures configuration group does not distinguish configurations based on placement of disarticulated cephalic sclerites, as under non-exceptional preservational regimes these could be confused through movement of sclerites, for example, in water currents).

Dataset Composition

Table 2 gives the number of moult specimens included in the dataset for each mode of moulting and generalised moult configuration, and summary metadata for the included specimens. Specimens spanned most currently named trilobite orders, though extensive high-level taxonomic uncertainty remains for the group (e.g., the suggested paraphyly of Ptychopariida; Adrain, 2011). All raw data is freely available in the associated Appendix data file.

Analyses

To test for associations between trilobite moulting behaviour and morphometry several targeted statistical analyses were performed. All analyses were performed and plots produced in R (Core Team, 2021) using RStudio (RStudioTeam, 2020) and the following additional packages: car (Fox and Weisberg, 2019); ColorBrewer (Brewer et al., 2003); ggplot2 (Wickham, 2016); ggpubr (Kassambara, 2020); jmv (Selker et al., 2021); mixtools (Benaglia et al., 2009); MorphoTools2 (Koutecký, 2015; Šlenker et al., 2022); stats (Core Team, 2021); tidyverse (Wickham et al., 2019); vegan (Oksanen et al., 2020). All analyses were performed on morphometric data of specimens grouped into both mode of moulting and generalised moult configuration (see Table 1). Descriptive statistics were produced for all morphometric variables.

Multivariate morphometric analyses were performed to determine whether specimens showing the same moulting behaviours grouped together in

morphospace. These consisted of both Principal Components Analyses (PCA) using a correlation matrix and Non-Metric Multidimensional Scaling (NMDS) analyses. PCA is traditionally used for biological morphometric analyses but cannot include data entries that contain missing information as it uses a Euclidean distance metric (Koutecký, 2015); this is unfortunately the case for this dataset, and frequently for fossil data. NMDS analysis uses alternative distance metrics (Buttigieg and Ramette, 2014), and represents a non-parametric alternative to PCA that can often be suitable for biological data due to their frequent violation of normality; these were therefore performed with all data included as a comparison to PCA. However, NMDS is not ideal in isolation because analyses can become stuck within local dataset minima, and it is not as informative as PCA because it cannot provide a breakdown of the influence of the original variables on the results. NMDS analyses produced Euclidean stress values of 0.12-0.13, which is considered suitable for reliable inference (Buttigieg and Ramette, 2014). NMDS analyses included all 617 specimens, while for PCA the total body length and pygidial length and width variables were removed due to their high proportions of incomplete data. With subsequent removal of incomplete data entries, this left 273 specimens for PCA. An eigenvector plot was produced to show the influence of the original measurement variables on the PCA morphospace. Ellipses on the PCA and NMDS plots represent the regions where new independent observations will fall with a 0.95 probability level. Following NMDS, non-parametric ANOSIM analyses were performed to test whether the dissimilarity in morphometry between each moulting group was greater than within each group (i.e., whether the moulting groupings would naturally group together based on morphometry; Buttigieg and Ramette, 2014).

Differences in average thoracic tergite number and each measurement variable associated with moulting behaviour were tested for using Kruskal-Wallis chi-squared analyses. Post-hoc Wilcoxon pairwise analyses were performed when a significant Kruskal-Wallis result was obtained. Multivariate Analysis of Covariance (MANCOVA) tests were used to explore the impact moulting behaviour had (the independent variable) on each morphometry variable (the dependent variable), while controlling for all other variables (the covariates). Controlling for all covariates simultaneously removed any association between the dependent variable and the remaining body proportion covariates, so that the only signal would be the impact on the dependent variable by the independent variable, without being confounded by effects of the covariates (e.g., if body length also impacts thoracic length, controlling for body length allows direct testing of the impact of moulting behaviour on thoracic length). Scatter plots with linear regressions predicted by the MANCOVA models were produced to visualise any differences between the moulting groups. A significance threshold of $a = 0.05$ was used throughout the analyses, though all relevant p values are reported for interrogation.

The distributions of data present were explored through qualitative interpretation of the linear regression plots and morphospace plots previously mentioned, followed by production of histograms for each variable. The fit of each dataset variable to a single distribution or a multiple mixed set of overlapping distributions was analysed using an iterative expectation-maximisation (EM) algorithm method, and its resulting distribution models and log-likelihood values (Benaglia et al., 2009). The less negative the log-likelihood figure at convergence of the estimate, the better the distribution model from the EM algorithm fits the data.

RESULTS

Dataset Moulting Variability is High

As fully detailed in Drage (2019a), interspecific moulting variability in the dataset is high. However, most specimens are preserved within the cephalic suture configuration group (469 specimens). Inversions of exoskeletal sclerites (including Salter's and cephalic sutures + inversion configurations) are generally less common in the dataset (55 specimens total). Moults manifesting as hybrids between the Sutural Gape and Salter's modes of moulting (the hybrid mode) showed the same occurrence frequency as inversions (55 specimens).

Moulting Behaviours are not Distinguished by Morphospace Occupation

Variance in PC1 of the PCA plots (Figure 3A-C) can be explained by differences in anterior cranidial width (tr.), cranidial length (sag.), cephalothoracic joint width (tr.), thoracic width (tr.), and partially thoracic length (sag.); that is, all included continuous measurement variables. Variance in PC2 (Figure 3A-C) can be explained almost entirely by thoracic tergite count, and partially by thoracic length (sag.). This difference in loading reflects the fact that all size variables are continu-

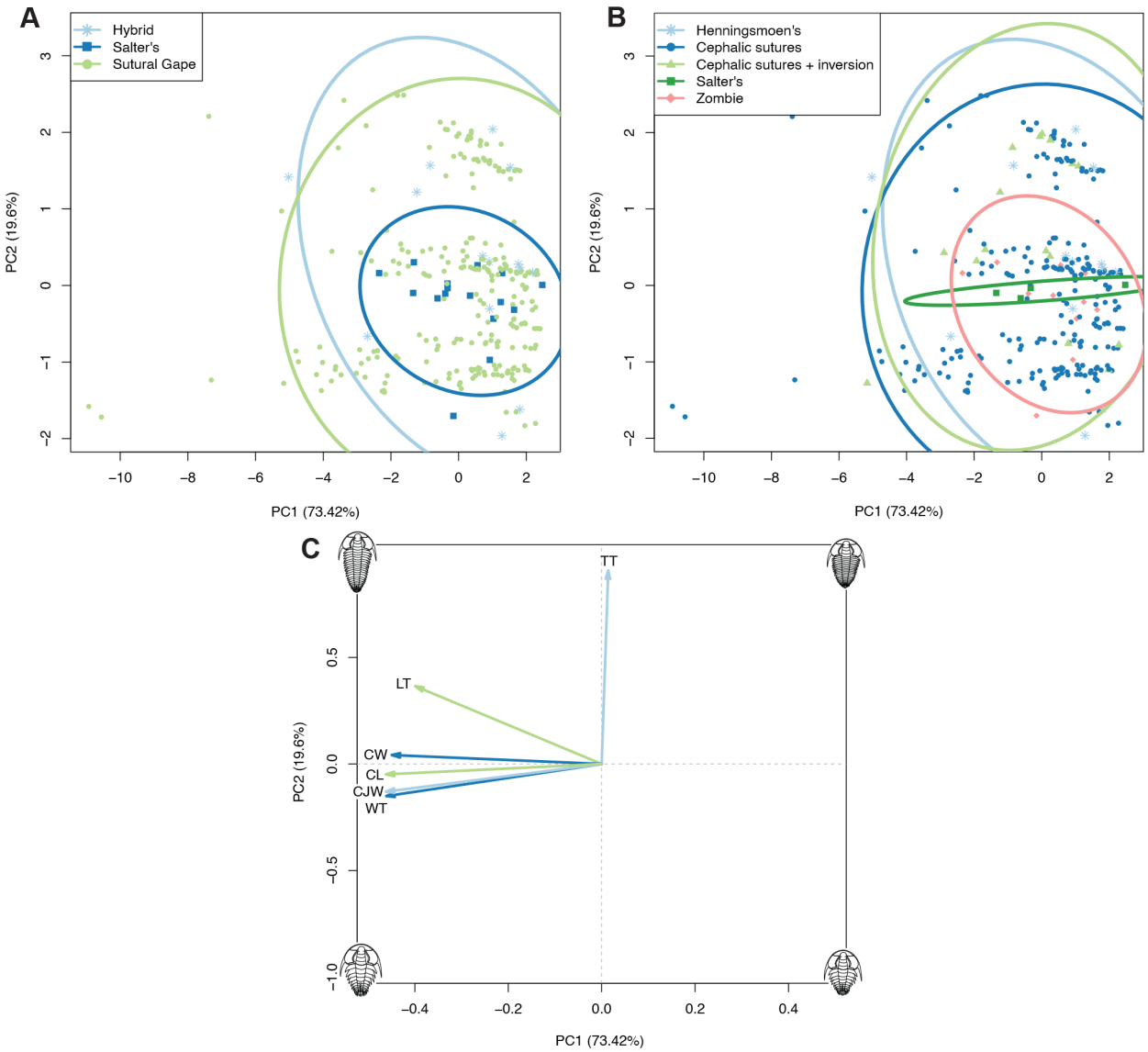

FIGURE 3. Principal Components Analysis plots with specimens grouped by mode of moulting (A) or generalised moult configuration (B) (see legends). Plot C shows the contributions of the dataset variables to the morphospace in A and B; directionality of each arrow represents how it varies across the morphospace, and length of each arrow represents its comparable impact on the morphospace. TT: thoracic tergite number, LT: thoracic axial length, WT: thoracic maximum width, CW: cranidial width, CL: cranidial axial length, CJW: cephalothoracic joint width.

ous metric measurements and covary due to their strong correlations with body length, and thoracic tergite count is a meristic trait and not immediately dependent on body length. Similarly, the slight covariance between thoracic tergite count and thoracic length, implied by their joint loading on PC2, is unsurprising given these are measures of similar, though not identical, morphological information (i.e., 'length' of the thorax). Dataset variation is represented by PC1 at 73% and PC2 at 20% (Figure 3A, B), leaving only 7% variation explained by the subsequent PCs. The PCA plots suggest no difference in the region of morphospace occupied by the different modes of moulting (Figure 3A) or generalised moult configurations (Figure 3B), as the ellipses are nested within each other. The NMDS plots support this finding, with the mode of moulting (Figure 3A) and generalised moult configuration (Figure 3B) group ellipses also being entirely nested. These results show that the different mode of moulting and generalised moult configuration groups cannot be distinguished based on their overall morphometries. ANOSIM tests support this, being non-significant for both mode (R =−0.0541, p

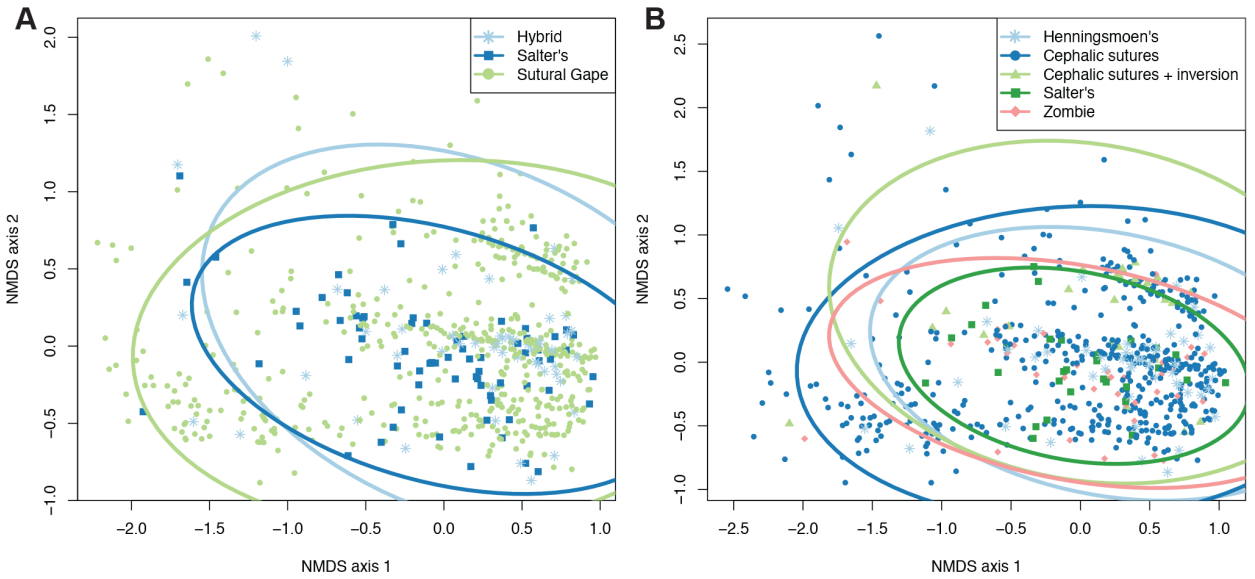

FIGURE 4. NMDS analysis plots with specimens grouped by mode of moulting (A) or generalised moult configuration (B) (see legends).

= 0.856) and configuration (R =−0.0632, p = 0.928), supporting the nesting of ellipses in the NMDS analyses and confirming that there is no significant difference between the moult groupings.

The PCA plots do suggest that Salter's mode of moulting (Figure 3A) and its corresponding generalised moult configurations (Salter's and Zombie configurations; Figure 3B) occupy a smaller region of morphospace than the other moulting groupings. This suggests a restricted range of morphometries for trilobites using Salter's mode, particularly in their number of thoracic tergites (along the PC2 axis) and their thoracic length (split between PC1 and 2 axes), this latter likely as thoracic length is related to tergite number (Figure 3C). The Zombie configuration grouping showed similar variation, though Salter's configuration was even more restricted in thoracic tergite number and length variation (Figure 3B). This smaller morphospace area occupation is not solely an artefact of the PCA sample sizes of these groupings, because other groupings in the plots have equivalent sample sizes. However, the NMDS plots, which include the total dataset sample, do not appear to support this result (Figure 4), with all groupings showing similar extents of variation in their areas of morphospace occupied; this may be related to the mapping procedure of NMDS, or the inclusion of additional specimens giving the groups more comparable spreads.

Thoracic Tergite Number and Length Are Significantly Different for Generalised Moult Configurations

Sutural Gape mode specimens had a mean average of 12 thoracic tergites and Salter's mode 11 tergites, with their medians both being 11 tergites, though the median for the hybrid mode was slightly higher at 13 tergites (Table 3, Figure 5A). However, there was no significant difference in thoracic tergite number when comparing mode of moulting groups (Table 3; Kruskal-Wallis: χ^2 = 18.412, p = 0.243). In contrast, the median number of thoracic tergites significantly differed between the generalised moult configuration groups (Table 4), demonstrated by a significant Kruskal-Wallis chi-squared test (χ^2 = 2.828, p = 0.00103). Moult specimens in the cephalic sutures + inversion group are responsible for this significant result, as evidenced by post-hoc Wilcoxon pairwise tests that were significant for this group when paired with all other configuration groupings (Henningsmoen's p = 0.00690, cephalic sutures p = 0.00077, Salter's p = 0.00188, Zombie p = 0.00053; no other pairings significant). The cephalic sutures + inversion group had a higher thoracic tergite count, with a mean of 15 and median of 17, compared to a mean of 12 for all other groupings (and 10 for Zombie configuration; Table 4, Figure 5B). Box plots of thoracic tergite number do show three major areas of clustering for the Sutural Gape mode of moulting, with the most extreme slightly skewing the results towards

TABLE 3. Descriptive statistics for the dataset, displaying the mean, standard deviation, and median values for each morphometry variable, grouped by mode of moulting. The hybrid mode of moulting represents moult specimens in Henningsmoen's configuration, with both the cephalic moulting sutures and the cephalothoracic joint opened.

Mode of moulting	Morphometry variable	Mean (mm)	Standard deviation	Median (mm)
Sutural Gape	thoracic tergite #	12	4.2	11
	thoracic width	22.4	14.8	17.4
	thoracic length	18.1	12.1	15.7
	cephalothoracic joint width	21.3	13.8	16.9
	anterior cranidial width	13.4	9.8	10.8
	cranidial length	13.7	8.6	11.2
	pygidial width	16.8	16.1	10.8
	pygidial length	10.1	10.1	5.9
	total body length	39.2	25.5	31.1
Salter's	thoracic tergite #	11	2.6	11
	thoracic width	22.8	11.3	21.2
	thoracic length	20.2	10.8	18.1
	cephalothoracic joint width	20.9	11.7	18.8
	anterior cranidial width	11.7	4.9	10.6
	cranidial length	13.0	6.8	11.6
	pygidial width	17.4	10.5	15.8
	pygidial length	10.1	7.7	7.5
	total body length	40.2	22.6	35.0
Hybrid	thoracic tergite #	12	3.9	13
	thoracic width	20.4	13.0	15.7
	thoracic length	19.9	17.7	14.0
	cephalothoracic joint width	22.8	31.1	14.9
	anterior cranidial width	11.2	7.1	8.7
	cranidial length	11.7	7.7	9.8
	pygidial width	13.3	11.8	9.0
	pygidial length	7.59	7.2	5.6
	total body length	32.3	22.8	24.6

a high number of tergites (Figure 5A), but this is not reflected in the group averages. The extreme positive cluster seen for the Sutural Gape mode in the boxplot (Figure 5A) seems more driven by the high tergite number for the cephalic sutures + inversion group, as the cephalic sutures configuration group has a confidence range with a lower top-end value (Figure 5B) compared to the Sutural Gape mode (Figure 5A). These findings all support that the significant results suggesting differences in thoracic tergite number are entirely due to the cephalic sutures + inversion configuration group, rather than a broad signal in the dataset. Although, tergite number box plots (Figure 5) may indicate a porous upper limit to the number of thoracic tergites for trilobites showing Salter's and the hybrid modes of moulting (and their constituent generalised moult configurations), as the numbers of specimens showing more than about 13 thoracic tergites for these groupings are extremely small.

As for thoracic tergite number, median thoracic length was significantly different between generalised moult configuration groupings (Kruskal-Wallis: χ^2 = 12.137, p = 0.0164), but not between modes of moulting (χ^2 = 2.845, p = 0.241). This again results from the cephalic sutures + inversion configuration group (Wilcoxon, p = 0.043 with cephalic sutures and Henningsmoen's configurations; no other pairings significant), with the inversion group having a thorax with a mean length of 23.7 mm compared to 17.7 mm and 18.0 mm for the Henningsmoen's and cephalic sutures groups, respectively (with the other two configura-

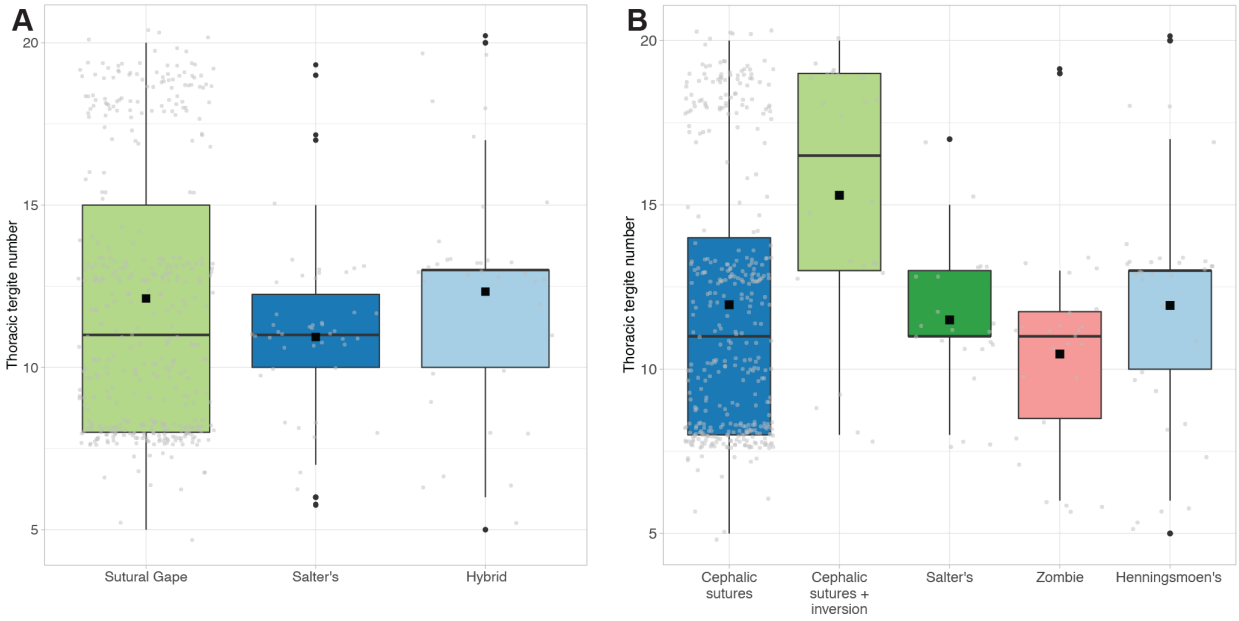

FIGURE 5. Box plots displaying mean (black square) and median (horizontal black line) average thoracic tergite number for each mode of moulting group (A) and generalised moult configuration (B). Grey jitter shows the plotted points comprising the boxes (jitter spread across the x-axis is purely for visualisation), and black points show suggested outliers.

tions having means of 20.3 and 20.1 mm). The similar results for the thoracic tergite number and length variables can be explained by the presumable co-dependence of the two, with a higher number of thoracic tergites generally associated with a longer thorax, and vice versa. However, this positive association does not hold for all moult groupings (Table 3); for example, specimens showing Salter's mode of moulting generally had a longer thorax in comparison to their thoracic tergite count (though this result is not statistically significant). Mode of moulting and generalised moult configuration were also determined to have a significant impact on thoracic length variance based on a MANCOVA test (p = 0.0354 for modes, p = 0.0210 for configurations).

Pygidial Width is Significantly Different for Moult Configurations

Median pygidial width was also found significantly differ between both mode of moulting groups (Kruskal-Wallis: χ^2 = 7.849, p = 0.0198) and generalised moult configuration groups (χ^2 = 12.703, p = 0.0128). For the mode of moulting groups this appears to result from the pairings of the Salter's mode group (Wilcoxon: Sutural Gape and Hybrid both p = 0.0260), with Salter's mode having a mean pygidial width of 17.4 mm compared to 16.8 mm for Sutural Gape and 13.3 mm for the hybrid mode (Table 4). When interrogating the generalised moult configuration group result, only the cephalic sutures + inversion group was found to have a significantly different pygidial width to other configurations (Wilcoxon: Salter's p = 0.0430, Zombie p = 0.00560; no other pairings significant). The inversion group had a narrower pygidium than these groups, at a mean of 11.0 mm compared to 16.7 mm and 17.9 mm, respectively, for the Salter's and Zombie configuration groups. Additionally, both mode of moulting and generalised moult configuration were suggested to have a significant impact on pygidial width variance based on MANCOVA tests (p = 0.0109 for modes, p = 0.0361 for configurations). This significant result is made clear by a scatterplot based on the MANCOVA model, with the linear regression lines clearly differing for the Sutural Gape and Salter's modes of moulting (Figure 6F).

Moulting is Unrelated to Most Other Morphometric Variables

The descriptive statistics suggest potential differences between the moulting groups for other morphometric variables (body length, pygidial length, cephalothoracic joint width, thoracic width, anterior cranidial width, cranidial length). For example, the median averages suggest specimens showing Salter's mode of moulting were generally

TABLE 4. Descriptive statistics for the dataset, displaying the mean, standard deviation, and median values for each morphometry variable, grouped by generalised moult configuration.

Generalised moult configuration	Morphometry variable	Mean (mm)	Standard deviation	Median (mm)
Cephalic sutures	thoracic tergite #	12	4.1	11
	thoracic width	22.4	14.9	17.2
	thoracic length	18.0	12.3	15.5
	cephalothoracic joint width	21.3	13.9	16.8
	anterior cranidial width	13.4	9.9	10.7
	cranidial length	13.8	8.7	11.2
	pygidial width	17.1	16.1	11
	pygidial length	10.2	10.2	6.0
	total body length	39.5	25.9	30.8
Cephalic sutures + inversion	thoracic tergite #	15	4.0	17
	thoracic width	21.5	12.6	18.3
	thoracic length	23.7	13.0	22.3
	cephalothoracic joint width	21.5	13.2	17.8
	anterior cranidial width	13.7	7.1	13.8
	cranidial length	14.0	9.5	11.0
	pygidial width	11.0	13.0	5.4
	pygidial length	7.0	7.5	4.5
	total body length	33.1	12.9	33.2
Henningsmoen's	thoracic tergite #	12	3.8	13
	thoracic width	20.4	13.3	15.4
	thoracic length	17.7	16.0	12.8
	cephalothoracic joint width	23.0	32.1	14.6
	anterior cranidial width	10.8	6.7	8.7
	cranidial length	10.8	5.4	9.7
	pygidial width	13.8	12.2	9.2
	pygidial length	7.8	7.5	5.7
	total body length	31.7	23.0	24.2
Salter's	thoracic tergite #	12	2.1	11
	thoracic width	23.3	9.0	24.3
	thoracic length	20.3	7.9	21.3
	cephalothoracic joint width	21.0	8.7	24.5
	anterior cranidial width	12.9	5.1	12.7
	cranidial length	12.7	5.6	12.2
	pygidial width	16.7	9.0	15.5
	pygidial length	8.7	6.5	6.5
	total body length	39.4	16.0	42.9

larger, and those showing the hybrid mode were generally smaller (Table 3). However, these remaining morphometric variables do not show statistically significant differences between mode of moulting or generalised moult configuration groups, based on Kruskal-Wallis tests. Further, MANCOVA tests indicate that both mode of moulting and generalised moult configuration had no significant impact on these morphometric variables, suggesting that these are unrelated to moulting behaviour. Scatterplots based on the MANCOVA models exemplify this lack of significant difference

TABLE 4 (continued).

Generalised moult configuration	Morphometry variable	Mean (mm)	Standard deviation	Median (mm)
	thoracic tergite #	11	2.9	11
	thoracic width	22.5	12.9	20.4
	thoracic length	20.1	12.8	16.6
	cephalothoracic joint width	20.8	13.4	15.4
Zombie	anterior cranidial width	11.1	4.7	9.9
	cranidial length	13.2	7.4	10.3
	pygidial width	17.9	11.4	16.4
	pygidial length	10.9	8.3	8.6
	total body length	40.5	25.2	33.7

between the moulting groups for these variables (Figure 6A-C, E, H). These plots generally show a single linear positive correlation, indicating these body proportions increase in size linearly with body length, rather than having multimodal distributions or the moulting groups showing differing slopes. This strong positive correlation is consistent with existing traditional analyses of trilobite growth (e.g., Palmer, 1957; Hughes and Chapman, 1995; Holmes et al., 2021).

Multimodal Distribution of Results?

Despite the lack of clear difference in morphospace occupation of the different moulting groups, the PCA plots (Figure 3) suggest a potential non-unimodal distribution of the data. There are three distinct clusters of points observable in the PCA morphospace, separated primarily along PC2, and which appear to cross the moulting groupings rather than being related to moulting behaviour (see particularly Figure 3B). The NMDS plots show the same three clusters of points, again apparently unrelated to moulting group (see particularly Figure 4B). This clustering indicates a trimodal distribution (three overlapping unimodal distributions) in the total dataset. Additionally, at least two clusters of points can be seen in several of the linear regression scatterplots, including for at least thoracic length (Figure 6D), pygidial length (Figure 6G), and pygidial width (Figure 6F); this also indicates bimodal or trimodal distributions for some of the morphometric measurements. Finally, similar data clustering can be observed in the thoracic tergite number boxplots (Figure 5), particularly for the Sutural Gape mode and cephalic sutures configuration, though the data also suggest this pattern may hold for the other moulting groupings if given greater sampling.

Further exploration of distribution patterns in the dataset through interpretation of histograms suggests a right-skewed unimodal distribution for all continuous morphometric measurements, and only a potential multimodal distribution for thoracic tergite number (Figure 7C). EM algorithm analysis (Benaglia et al., 2009) supports this result for all variables, with all except for thoracic tergite number appearing to best fit a unimodal right-skewed distribution (e.g., Figure 7A; log-likelihood at convergence for two and three distribution peaks = -731 to -1035). Pygidial length and width (and to an extent cranidial width and length) show a slightly better fit with a bimodal distribution (with two means predicted by the EM algorithm) than the other variables (e.g., Figure 7B). However, a right-skewed unimodal distribution remains the best fit for these variables, as is clear from their histograms (Figure 7B underlying histogram). For thoracic tergite number, the EM algorithm analysis suggests a trimodal distribution (three overlapping unimodal distributions, each with a different mean) best fits the data (Figure 7C; log-likehood = -567.809), with a bimodal distribution having a poorer fit (log-likehood = -637.807). A trimodal distribution for the tergite number variable fits the three data clusters described from the morphospace plots (Figures 3 and 4) and boxplots (Figure 5), suggesting this represents a true signal in the dataset. The three morphospace clusters appear to correspond with the three distribution peaks predicted by the EM algorithm, because the clusters are indeed separated along PC2 (representing mainly thoracic tergite number variation) rather than PC1 (most other variables) (see Figure 7D).

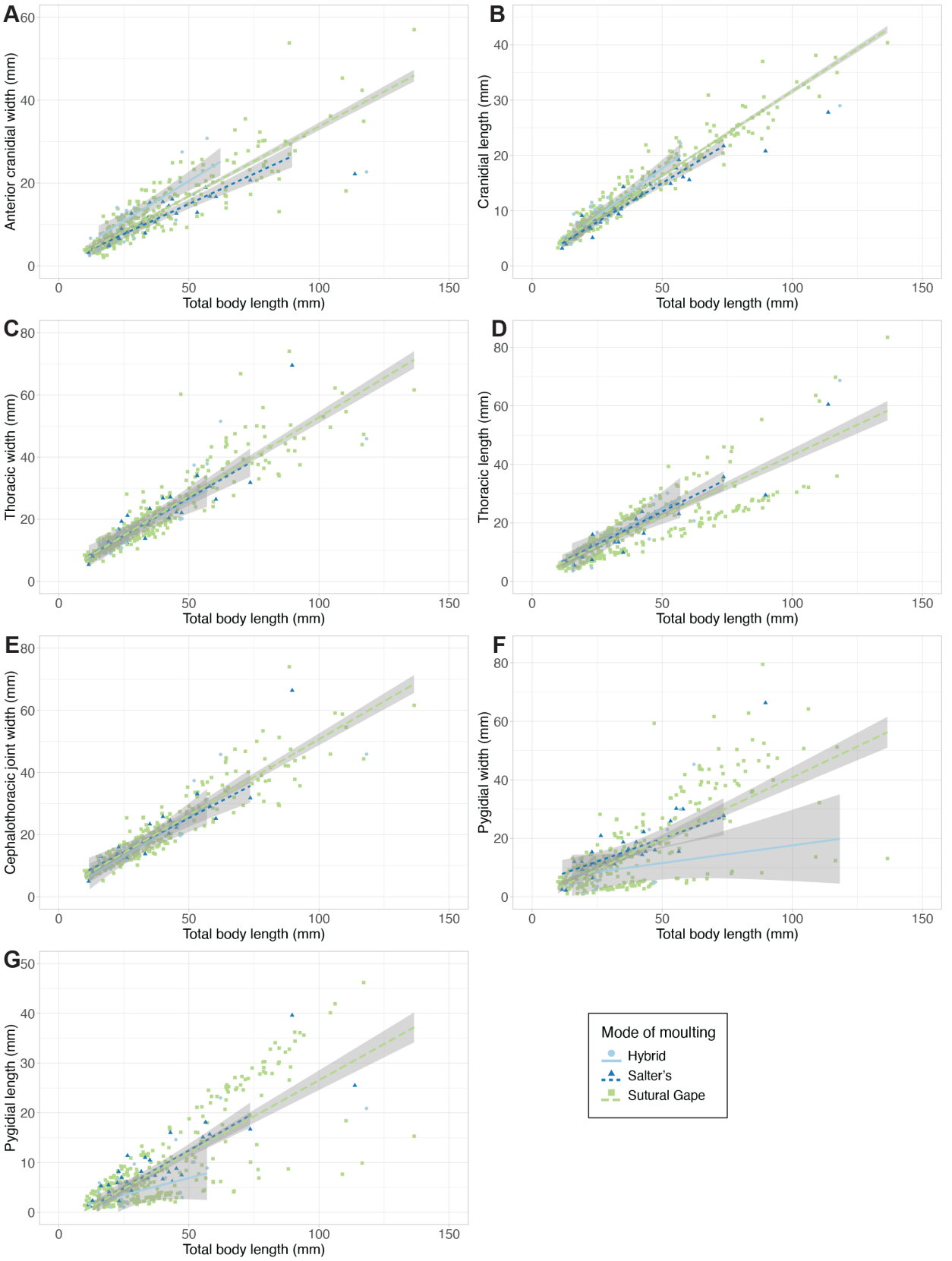

FIGURE 6. Scatterplots of the total dataset, for each metric morphometry variable. Data is grouped by mode of moulting (see legend). Linear regression lines represent the MANCOVA analysis models (see text).

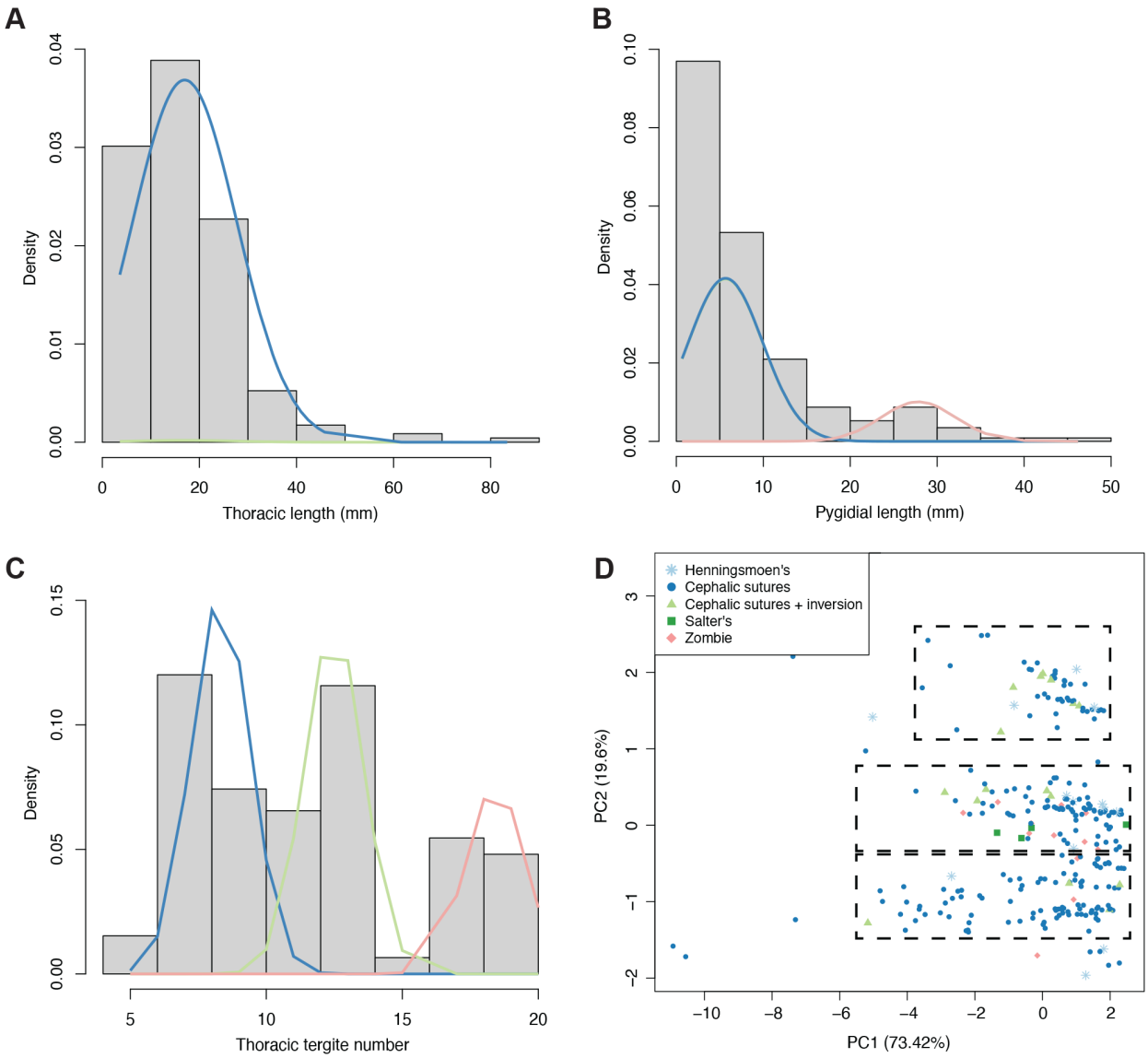

FIGURE 7. Histograms of notable variables within the dataset (using only complete data entries), with plotted EM algorithm-calculated distributions. A: thoracic axial length histogram, with two estimated distributions. B: pygidial axial length histogram, with three estimated distributions; two (blue and green lines) are exactly overlapping, indicating they represent the same distribution. C: thoracic tergite number, with three estimated distributions. D: PCA plot, with specimens grouped by generalised moult configuration (see legend) and ellipses removed (original plot in Figure 3B); dashed black boxes roughly demonstrate the three major data clusters apparent in the morphospace.

DISCUSSION

Overall, the results of this morphometric study suggest that there is little association between morphometry and moulting behaviour in trilobites. Certain results suggest a morphometric difference between individuals employing different modes of moulting, in particular the Salter's mode group in PCA and NMDS analyses showing less variation than groups using the cephalic sutures (Figures 3 and 4). This may suggest that the Sutural Gape mode of moulting is feasible over a wider range of body morphometries. Further, the morphospace plots and thoracic tergite number boxplots (Figure 5) suggest that the Sutural Gape mode may dominate at high tergite numbers. It may also be the case that trilobite species that habitually used Salter's mode of moulting (particularly if resulting from fusion of the facial sutures) had a more constrained morphometry due to an evolutionary phenomenon like a phylogenetic bottleneck, as many of these species, though not all, belong to the

same suborder (Phacopina; Crônier, 2013; Drage, 2019a). However, the NMDS analyses show the moulting groups to be more similar in their extents of variation, so the PCA results may be partially related to the necessary exclusion of incomplete specimen data in these analyses.

Most morphometric variables in the dataset were unrelated to moulting. However, means and variances of pygidial width did appear to significantly differ between the moulting behaviour groupings. Pygidial width significance may be related to the major pygidial forms described for trilobites (see Whittington et al., 1997; Hughes, 2007), and these different forms might also explain the apparent multimodal distributions observed in scatterplots (Figure 6F and G). Isopygous and macropygous pygidia are as broad as, and occasionally broader than, the thorax, and therefore may be more difficult to extract through potentially smaller exuvial gapes created by the cephalic sutures during moulting compared to micropygous pygidia. Indeed, pygidia were found to be significantly broader in specimens showing Salter's mode of moulting compared to the Sutural Gape and hybrid modes (both of which use the cephalic sutures; Table 3). At a generalised moult configuration level, the cephalic sutures + inversion group had a significantly narrower pygidium in comparison to the broader pygidium seen in the Salter's and Zombie configuration groupings (Table 4). Histograms of separate morphometric measurements suggest that neither pygidium measurements are multimodally distributed with peaks corresponding to macro-micropygous forms, although a potential minor second distribution is interpretable from the EM algorithm analysis (Figure 7B). Based on these results, the multiple distributions observed for pygidium size in the dataset may be related to moulting behaviour differences, rather than just reflecting the different morphological forms (e.g., macro-, iso-, micropygous) known in trilobites.

Thoracic length means and variances were also significantly different between the moulting groups in the dataset. Moult specimens with only open cephalic sutures (Sutural Gape mode of moulting) appeared to have an overall shorter thorax (in fact, a generally smaller thorax in length and width) than those using the cephalothoracic joint during moulting (Salter's mode of moulting; Table 3), which may be for mechanistic reasons such as a longer thorax being easier to extract through a joint at the cephalothorax than a potentially thinner gap at the anterior of the cephalon. However, a stronger and clearer trend would be required for this interpretation to be convincing; the Kruskal-Wallis comparisons suggest it is only the cephalic sutures + inversion configuration specimens that significantly differ in thoracic length (being actually longer than Salter's mode and configuration; Table 4), and thoracic width does not show a significant signal. There was also a significant association between generalised moult configuration and thoracic tergite number, caused by the cephalic sutures + inversion configuration specimens having a higher number of tergites (Figure 5). Brandt (2002) suggested that an overall trend to decreased thoracic tergite numbers over trilobite evolutionary history (Hughes et al., 2001) might be related to fewer tergites being less risky for moulting, though Hopkins and To (2022) found only a trend of decreasing tergite number range, not average. The minor association between moulting behaviour and tergite number reported here does not seem to bear out the suggestion of Brandt (2002), with the cephalic sutures + inversion group unlikely to be much riskier than the highly common cephalic sutures group. The results here may be due to the reasonably small sample size for the cephalic sutures + inversion group (25 specimens), though the otherwise lack of association between tergite number and moulting behaviour is probably not sampling-related due to the generally large sample sizes. Given this absence of a broad signal regarding thoracic length and tergite number in the dataset, a potential explanation is that this result may be related only to mechanical mechanisms such as articulation strength. This result is also the opposite to that found by Drage et al. (2023a), in which *Estaingia bilobata* moults with longer bodies were often preserved with only cephalic sutures open (cephalic sutures configuration), potentially suggesting that better developed articulations with increasing size reduced the incidence of Salter's mode of moulting. However, *Aulacopleura koninckii* Barrande, 1846, and *Dalmanitina* species transition from the Sutural Gape mode of moulting to Salter's mode of moulting (through ankylosis of the facial sutures) at or close to the onset of holaspis, when the thorax was comparably long with more numerous segment articulations (Drage et al., 2018b; Esteve and Hughes, 2023). These contrasting results suggest that this thoracic morphometric trend cannot be applied across this diverse group, and perhaps reflects lower taxonomic level biomechanical or ontogenetic differences. Further work on variable segment proportions and on whether articulation strength varies with size would be of interest regarding these findings.

The apparent non-unimodal distributions present for some variables (pygidial length and width, thoracic length) within the dataset raise additional interesting considerations about potential morphological constraints in trilobites. A unimodal skewed (rather than normal) distribution, which we see for most morphometric variables in this dataset (e.g., Figure 7A), is common and can be informative for continuous measurements of biological systems (e.g., Church et al., 2019), particularly for body size (Kozłowski and Gawelczyk, 2002), though this usually applies to organisms demonstrating continuous growth, rather than the stepwise growth following a moult cycle in arthropods. It is interesting that clustering in the linear regression scatterplots (Figure 6) and the EM algorithm results (Figure 7B) suggest the potential for a bimodal distribution in pygidium measurements. As noted above, these clusters, or distribution peaks, might represent different morphometric trajectories for groups with highly differing morphologies or ontogenetic pathways, though this would benefit from future attention at the species-level to thoroughly address broad-scale trends in this area. The clear multimodal distribution for thoracic tergite number (Figure 7C) suggests that trilobites tend to congregate at certain numbers of thoracic tergites within this dataset, with more trilobites with *c.* 8, 12, and 18 thoracic tergites than between these numbers (Figure 7). This is interesting because of the highly complex and varied segmentation patterns occurring within the Trilobita (e.g., see Hughes, 2003). Apparent stability of these thoracic tergite numbers could be explained by many factors affecting broad-scale evolution that are difficult to unpick, including morphological, behavioural, and ecological factors. Hughes et al. (2001) discussed convergence on stable thoracic tergite numbers as a broad-scale evolutionary pattern visible in trilobites. Hopkins and To (2022) have also recently demonstrated using a large dataset of trilobite tergite counts that the group showed a median of 17 tergites, and there was long-term convergence on this number, demonstrating overall stability in this variable. Tergite number stability is likely only tangentially related to moulting behaviour because a broad-scale signal with thoracic tergite count is not apparent in the dataset (only for the cephalic sutures + inversion configuration). Peaks in thoracic tergite number, such as that seen in this dataset, could also be explained by evolutionary bottlenecks, in which tergite number is more controlled by phylogenetic descent than by adaptation. Stabilisation of tergite number in trilobites could thereby result from a constraint on this number in early representatives of the group, and through time sufficient morphological adaptation took place around this tergite number to cause alteration of this characteristic to be evolutionarily unsuccessful. Indeed, Hughes (2003) noted that early-diverging trilobite groups displayed high variation in thoracic tergite number, and derived clades showed more stable numbers of tergites, with higher taxonomic ranks in particular showing more stable tergite numbers later in trilobite evolutionary history (Hughes et al., 2001); a finding that also seems to be supported by the large dataset of Hopkins and To (2022).

Moult configurations with exoskeletal inversion, both of cephalic sclerites and the complete cephalon (Salter's configuration), were generally uncommon in the dataset, potentially suggesting these were a rarer occurrence in Trilobita than may be highlighted in certain species (Speyer, 1985; Whittington, 1990). Inversion has been suggested to occur through dorsal flexure or partial enrolment of the individual during moulting (Whittington, 1990; McNamara and Rudkin, 1984; Daley and Drage, 2016; Drage, 2019a,b), for example in *Estaingia bilobata* (Drage et al., 2018a), and so its rarity here suggests many trilobites may have remained unflexed during moulting. Nevertheless, changes in moulting behaviour through ontogeny described by Wang et al. (2021) may suggest that certain trilobite species did regularly employ flexure for moulting but that this was linked to their development. Alternatively, this may reflect a description bias of trilobite moult specimens. Interesting or unusual moult specimens may, in general, be preferentially figured within manuscripts, but when assessing the bulk of historical museum specimens these may be less common in number than expected.

Additionally, taphonomic processes, notably biostratinomy, could impact the interpretation of moult fossils. Several named moult configurations (see Drage et al., 2018a) are single disarticulations apart, sometimes differing only in the retaining of the integument connecting disarticulated cephalic structures (compare, for example, Harrington's and Nutcracker configurations). Therefore, in locations where burial does not swiftly follow moulting or death, and substantial decay and/or biostratinomic processes like current flow occur prior to burial, some configurations could be placed on a continuum; for example, Harrington's configuration being morphed into the Nutcracker configuration through the decay process. Wang et al. (2023) also raised

this concern, though suggested that the Somersault configuration, due to inversion of only the librigenae, represented a true biological signal. It is therefore important to follow established criteria for distinguishing moults, and to ensure preservation and geological context are considered (Henningsmoen, 1975; Daley and Drage, 2016). Additionally, it is for this reason that both mode of moulting and generalised moult configuration were analysed here – mode of moulting focuses solely on the major morphological structures involved in moulting, rather than on moulting behavioural differences causing minor differences in configuration preservation, and so may be more robust to taphonomic impacts. Further, the number of moult configurations analysed here was reduced ('generalised') from those named in Drage et al. (2018a), because their configurations were based on a sample preserved under exceptional conditions with little transportation prior to burial, and so presumably underwent a lesser impact of biostratinomy, compared to the broad-scale dataset analysed here that covers many preservational regimes. Direct testing of the impact of decay and biostratinomic impacts would be useful to future interpretations, particularly broad scale, of fossil arthropod moulting.

Finally, while this dataset includes specimens from most currently named trilobite orders (following Adrain, 2011) and Palaeozoic periods, broad-scale datasets such as this can be improved through targeted sampling of underrepresented groups. Here, this includes notably the order Proetida, and the Aulacopleurida, Lichida, Olenida, and Odontopleurida (see Table 2). The Cambrian and Ordovician, with high trilobite diversities and abundances (e.g., Foote, 1993; Westrop and Adrain, 1998; Webster, 2007), are well-represented in this dataset, though the Carboniferous and Permian are under-sampled, as also manifested in the paucity of proetids (Hopkins et al., 2023). Similarly, taxa recorded from the Global South tend to be underrepresented in the published literature and 'international' museum collections, and thereby in large and meta-dataset analyses; working with collaborators in these areas should be prioritised in future broad-scale data studies of arthropod moulting to prioritise the inclusion of these species.

CONCLUSIONS

This work presents the first large cross-group quantitative analysis exploring a potential link between trilobite moulting behaviour and morphometry. The dataset suggests some minor differences in morphometry between groups of specimens displaying different modes of moulting and preserving different generalised moult configurations. In particular, the apparent presence of a longer thorax with more articulations and a narrower pygidium in specimens showing open cephalic sutures + inversion, and potentially less variation in the morphology of specimens using Salter's mode of moulting. However, little association between most of the morphometry variables investigated and any other moulting grouping was detected. Further, although the sample size for the cephalic sutures + inversion configuration group was sufficient to be included in this study (at 25 specimens), more specimens (ideally approximately 100) would be required for the results to be considered conclusive, though this would be difficult due to the configuration's apparent rarity. Lastly, if there was a clear association, even minor, between morphometry and moulting behaviour in trilobites, we would not expect to see significant results with only one, reasonably rare, grouping of moult configurations. To be confident of any real biological association, we would require some suggestion of differing morphometry between the main modes of moulting; Sutural Gape and Salter's modes, and this was not seen.

The lack of clear morphometric association with other moulting groupings in the dataset is itself interesting, because we would expect morphology and key behaviours like moulting to interact and invoke changes in each other, particularly over long evolutionary timescales (Henningsmoen, 1975; Brandt, 2002). It raises the question of whether moulting behaviour variability in trilobites can be considered related to morphological aspects outside of the obvious existence or loss of physical moulting mechanisms, such as the facial sutures (Whittington, 1990; Drage, 2019a). There may be a minor association, as suggested by this morphometric study, however, other factors influencing morphology seem to have played larger roles in determining moulting behaviour variability. For example, it is possible that, rather than being directly related to morphometry, moulting behaviour interacted with morphological complexity, as Brandt (2002) suggested, such as the number of exoskeletal articulations and spinosity (the latter of which Whittington, 1990, suggested may be important as leverage during moulting). The thoracic tergite count results presented here do not necessarily bear this out, though broad-scale trends in trilobite spinosity, articulation strength,

and segment proportions deserve further exploration, and quantitative study of other complexity measures across groups could be consequently informative. Otherwise, this lack of strong morphometric signal suggests other aspects of trilobite evolutionary history that may have influenced moulting variability deserve attention, for example, phylogenetic relationships. Similarly, other ecological adaptations may have influenced the moulting process, such as a burrowing lifestyle and the physical stresses this places on the facial sutures (Esteve et al., 2021). This suggests that greater in-depth and holistic study on trilobites is required to understand the evolutionary impacts of their apparent moulting behaviour flexibility.

ACKNOWLEDGEMENTS

The author wishes to gratefully thank S. Pates and A.C. Daley for their long-standing constructive conversations on this work, and for providing comments on an earlier version of this manuscript. Additionally, two anonymous reviewers helped to improve this manuscript, and are gratefully acknowledged for their work. H. B. D. is funded by a Swiss National Science Foundation Sinergia grant (198691).

REFERENCES

Adrain, J.M. 2011. Class Trilobita Walch, 1771, 104–109. In Zhang, Z.-Q. (ed.), Animal biodiversity: An outline of higher-level classification and survey of taxonomic richness. Zootaxa, 3148:104. https://doi.org/10.11646/zootaxa.3148.1.15

Barrande, J. 1846. Notice Préliminaire sur le Système Silurien et les Trilobites de Bohême. Hirschfield, Leipzig.

Benaglia, T., Chauveau, D., Hunter, D.R., and Young, D. 2009. mixtools: An R package for analyzing finite mixture models. Journal of Statistical Software, 32:1–29. http://www.jstatsoft.org/v32/i06/

Boeck, C.P.B. 1827. Notiser til Laeren om Trilobiterne. Magazin for Naturvidenskaberen, 8:11–44.

Brandt, D.S. 2002. Ecydsial efficiency and evolutionary efficacy among marine arthropods: implications for trilobite survivorship. Alcheringa, 26:399–421. https://doi.org/10.1080/03115510208619264

Brewer, C.A., Hatchard, G.W., and Harrower, M.A. 2003. ColorBrewer in Print: A Catalog of Color Schemes for Maps. Cartography and Geographic Information Science, 30:5–32. https://doi.org/10.1559/152304003100010929 [R version 4.1.2].

Brünnich, M.T. 1781. Beskrivelse over Trilobiten, en Dyreslaegt og dens Arten, med en nye Arts aftegning. Nye Samling af det Kongelige Danske Videnskabers Selskabs Skrifter, 1:384–395.

Budil, P. and Bruthansova, J. 2005. Moulting in Ordovician dalmanitoid and acastoid trilobites of the Prague Basin. Preliminary observation. Geologica Acta, 11:373–383. https://doi.org/10.1344/105.000001385

Buttigieg, P.L. and Ramette, A. 2014. A guide to statistical analysis in microbial ecology: a community focused, living review of multivariate data analyses. FEMS Microbiology Ecology, 90:543–550. https://doi.org/10.1111/1574-6941.12437

Church, B.V., Williams, H.T., and Mar, J.C. 2019. Investigating skewness to understand gene expression heterogeneity in large patient cohorts. BMC Bioinformatics, 20:1–14. https://doi.org/10.1186/s12859-019-3252-0

Corrales-García, A., Esteve, J., Zhao, Y., and Yang, X. 2020. Synchronized moulting behaviour in trilobites from the Cambrian Series 2 of South China. Scientific Reports, 10:14099. https://doi.org/10.1038/s41598-020-70883-5

Crônier C. and Fortey, R.A.F. 2006. Morphology and ontogeny of an Early Devonian phacopid trilobite with reduced sight from southern Thailand. Journal of Palaeontology, 80:529–536. https://doi.org/10.1666/0022-3360(2006)80[529:MAOOAE]2.0.CO;2

Crônier, C. 2013. Morphological disparity and developmental patterning: contribution of phacopid trilobites. Palaeontology, 56:1263–1271. https://doi.org/10.1111/pala.12024

Daley, A.C. and Drage, H.B. 2016. The fossil record of ecdysis, and trends in the moulting behaviour of trilobites. Arthropod Structure & Development, 45:71–96. https://doi.org/10.1016/j.asd.2015.09.004

Drage, H.B. 2019a. Quantifying intra- and interspecific variability in trilobite moulting behaviour across the Palaeozoic. Palaeontologia Electronica, 1–39. https://doi.org/10.26879/940

Drage, H.B. 2019b. The evolution of exoskeleton moulting in Trilobita. PhD thesis, University of Oxford. https://ora.ox.ac.uk/objects/uuid:42af12f6-ff0c-41ca-b93c-8d1482f8c479

Drage, H.B., Holmes, J.D., García-Bellido, D.C., and Daley, A.C. 2018a. An exceptional record of Cambrian trilobite moulting behaviour preserved in the Emu Bay Shale, South Australia. Lethaia, 51:473–492. https://doi.org/10.1111/let.12266

Drage, H.B., Laibl, L., and Budil, P. 2018b. Postembryonic development of *Dalmanitina*, and the evolution of facial suture fusion in Phacopina. Paleobiology, 44:638–659. https://doi.org/10.1017/pab.2018.31

Drage, H.B., Vandenbroucke, T.R.A., Van Roy, P., and Daley, A.C. 2019. Sequence of post-moult exoskeleton hardening preserved in a trilobite mass moult assemblage from the Lower Ordovician Fezouata Konservat-Lagerstätte, Morocco. Acta Palaeontologica Polonica, 64:261–273. https://doi.org/10.4202/app.00582.2018

Drage, H.B., Holmes, J.D., García-Bellido, D.C., and Paterson, J.R. 2023a. Associations between trilobite intraspecific moulting variability and body proportions: *Estaingia bilobata* from the Cambrian Emu Bay Shale, Australia. Palaeontology, 66:e12651. https://doi.org/10.1111/pala.12651

Drage, H.B., Legg, D.A., and Daley, A.C. 2023b. Novel marrellomorph moulting behaviour preserved in the Lower Ordovician Fezouata Shale, Morocco. Frontiers in Ecology and Evolution, 11:1226924. https://doi.org/10.3389/fevo.2023.1226924

Du, K.-S., Ortega-Hernandez, J., Yang, J., and Zhang, X.-G. 2019. A soft-bodied euarthropod from the early Cambrian Xiaoshiba Lagerstätte of China supports a new clade of basal artiopodans with dorsal ecdysial sutures. Cladistics, 35:269–281. https://doi.org/10.1111/cla.12344

Esteve, J. and Hughes, N.C. 2023. Developmental and functional controls on enrolment in an ancient, extinct arthropod. Proceedings of the Royal Society B, 290:20230871. https://doi.org/10.1098/rspb.2023.0871

Esteve, J., Marcé-Nogué, J., Pérez-Peris, F., and Rayfield, E. 2021. Cephalic biomechanics underpins the evolutionary success of trilobites. Palaeontology, 64:519–530. https://doi.org/10.1111/pala.12541

Ewer, J. 2005. How the Ecdysozoan changed its coat. PLoS Biology, 3:e349. https://doi.org/10.1371/journal.pbio.0030349

Foote, M. 1993. Discordance and concordance between morphological and taxonomic diversity. Paleobiology, 19:185–204. https://doi.org/10.1017/S0094837300015864

Fortey, R.A. 2001. Trilobite systematics: the last 75 years. Journal of Paleontology, 75:1141–1151. https://doi.org/10.1666/0022-3360(2001)075%3C1141:TSTLY%3E2.0.CO;2

Fortey, R.A. and Owens, R.M. 1999. Feeding habits in trilobites. Palaeontology, 42:429–465. http://doi.org/10.1111/1475-4983.00080

Fortey, R.A. and Whittington, H. 1989. The Trilobita as a natural group. Historical Biology, 2:125–138. https://doi.org/10.1080/08912968909386496

Fox, J. and Weisberg, S. 2019. An R Companion to Applied Regression, Third Edition. Sage, Thousand Oaks, California. https://socialsciences.mcmaster.ca/jfox/Books/Companion/ [R version 3.1.2].

Henningsmoen, G. 1975. Moulting in trilobites. Fossils and Strata, 4:179–200.

Holmes, J.D., Paterson, J.R., and García-Bellido, D.C. 2021. Complex axial growth patterns in an early Cambrian trilobite from South Australia. Proceedings of the Royal Society B, 288:20212131. https://doi.org/10.1098/rspb.2021.2131

Hopkins, M.J. and To, R. 2022. Long-term clade-wide shifts in trilobite segment number and allocation during the Palaeozoic. Proceedings of the Royal Society of Biology B, 289:20221765. https://doi.org/10.1098/rspb.2022.1765

Hopkins, M.J., Wagner, P.J., and Jordan, K.J. 2023. Permian trilobites and the applicability of the "living fossil" concept to extinct clades. Frontiers in Ecology and Evolution, 11. https://doi.org/10.3389/fevo.2023.1166126

Hou, X., Williams, M., Gabbott, S., Siveter, D.J., Siveter, D.J., Cong, P., Ma, X., and Sansom, R. 2017. A new species of the artiopodan arthropod *Acanthomeridion* from the lower Cambrian Chengjiang Lagerstätte, China, and the phylogenetic significance of the genus. Journal of Systematic Palaeontology, 15:733–740. https://doi.org/10.1080/14772019.2016.1229695

Hughes, N.C. 2003. Trilobite tagmosis and body patterning from morphological and developmental perspectives. Integrative and Comparative Biology, 43:185–206. https://doi.org/10.1093/icb/43.1.185

Hughes, N.C. 2007. The evolution of trilobite body patterning. Annual Review of Earth and Planetary Sciences, 35:401–434. https://doi.org/10.1146/annurev.earth.35.031306.140258

Hughes, N.C. and Chapman, R.E. 1995. Growth and variation in the proetide trilobite *Aulacopleura konincki* and its implications for trilobite palaeobiology. Lethaia, 28:333–353. http://doi.org/10.1111/j.1502-3931.1995.tb01824.x

Hughes, N.C., Chapman, R.E., and Adrain, J.M. 2001. The stability of thoracic segmentation in trilobites: a case study in developmental and ecological constraints. Evolution & Development, 1:24–35. https://doi.org/10.1046/j.1525-142x.1999.99005.x

Hughes, N.C., Macquaker, J.H.S., and Huff, W.D. 2014. The depositional environment and taphonomy of the Homerian *Aulacopleura* shales fossil assemblage near Lodënice, Czech Republic (Prague Basin, Perunican microcontinent). Bulletin of Geosciences, 89:219–38. https://doi.org/10.3140/bull.geosci.1414

Kassambara, A. 2020. ggpubr: 'ggplot2' Based Publication Ready Plots. https://CRAN.Rproject.org/package=ggpubr [Version 0.4.0].

Kielan, Z. 1960. Upper Ordovician trilobites from Poland and some related forms from Bohemia and Scandinavia. Palaeontologia Polonica, 11:1–198.

Koutecký, P. 2015. MorphoTools: a set of R functions for morphometric analysis. Plant Systematics and Evolution, 301:1115–1121. https://doi.org/10.1007/s00606-014-1153-2

Kozłowski, J. and Gawelczyk, A.T. 2002. Why are species' body size distributions usually skewed to the right? Functional Ecology, 16:419–432. https://doi.org/10.1046/j.1365-2435.2002.00646.x

Lu, Y.-H. 1950. On the genus *Redlichia* with description of its new species. Geological Review, 15:157–169.

Lu, Y.H., Zhu, Z.L., Qian, Y.Y., Lin, H.L., Zhou, Z.Y., and Yuan, K.X. 1974. Bio-environmental control hypothesis and its application to Cambrian biostratigraphy and palaeozoogeography [in Chinese, with English summary]. Memoir of the Nanjing Institute of Geology and Palaeontology, Academia Sinica, 5:27–110.

Mángano, M.G., Ortega-Hernández, J., Piñuela, L., Buatois, L.A., Rodríguez-Tovar, F.J., and García-Ramos, J.C. 2020. Trace fossil evidence for infaunal moulting in a Middle Devonian non-trilobite euarthropod. Scientific Reports, 10:5316. https://doi.org/10.1038/s41598-020-62019-6

McNamara, K.J. and Rudkin, D.M. 1984. Techniques of trilobite exuviation. Lethaia, 17:153–173. https://doi.org/10.1111/j.1502-3931.1984.tb01722.x

Moysiuk, J. and Caron, J.-B. 2023. A quantitative assessment of ontogeny and molting in a Cambrian radiodont and the evolution of arthropod development. Paleobiology, online access:1–16. https://doi.org/10.1017/pab.2023.18

Oksanen, J., Blanchet, F.G., Friendly, M., Kindt, R., Legendre, P., McGlinn, D., Minchin, P.R., O'Hara, R.B., Simpson, G.L., Solymos, P., Stevens, M.H.H., Szoecs, E., and Wagner, H. 2020. vegan: Community Ecology Package. https://CRAN.R-project.org/package=vegan [Version 2.6-2].

Olempska, E., Mundy, D.J.C., and Zatoń, M. 2023. Cryptic moulting behaviour of some Carboniferous Ostracoda. Papers in Palaeontology, 9:e1519. https://doi.org/10.1002/spp2.1519

Palmer, A.R. 1957. Ontogenetic development of two olenellid trilobites. Journal of Palaeontology, 31:105–128.

Park, T.Y. and Choi, D.K. 2011. Constraints on using ontogenetic data for trilobite phylogeny. Lethaia, 44:250–254. https://doi.org/10.1111/j.1502-3931.2011.00279.x

Piccoli, A.D., Carbonaro, F.A., Sousa, F.N., and Ghilardi, R.P. 2021. Moulting patterns in trilobite from the Devonian of the Paraná Basin. Terr@Plural, 15:1–8. https://revistas.uepg.br/index.php/tp/article/view/17837

Pocock, K.J. 1964. *Estaingia*, a new trilobite genus from the Lower Cambrian of South Australia. Palaeontology, 7:458–471.

Portlock, J.E. 1843. Report on the Geology of the County of Londonderry and of parts of Tyrone and Fermanagh. Longman et al, London.

R Core Team. 2021. R: A language and environment for statistical computing. R Foundation for Statistical Computing, Vienna, Austria. http://www.R-project.org/.

R Studio Team. 2020. RStudio: Integrated Development for R. RStudio, PBC, Boston, Massachusetts. https://posit.co/products/open-source/rstudio/. [RStudio version 2021.09.0+351 "Ghost Orchid" Release for macOS].

Richter, R. 1856. Beitrag zur Paläontologie des Thüringer Waldes. Erster Theil. Denkschriften der kaiserlichen Akademie der Wissenschaften, mathematisch – naturwissenschaftlichen Klasse, 11:87–138.

Schindelin, J., Arganda-Carreras, I., Frise, E., Kaynig, V., Longair, M., Pietzsch, T., Preibisch, S., Rueden, C., Saalfeld, S., Schmid, B., Tinivez, J.-Y., White, D.J., Hartenstein, V., Eliceiri, K., Tomancak, P., and Cardona, A. 2012. Fiji: an open-source platform for biological-image analysis. Nature Methods, 9:676–682. https://doi.org/10.1038/nmeth.2019

Selker, R., Love, J., Dropmann, D., and Moreno, V. 2021. jmv: The 'jamovi' analyses. https://CRAN.Rproject.org/package=jmv [Version 2.3.4].

Šlenker, M., Koutecký, P., and Marhold, K. 2022. MorphoTools2: an R package for multivariate morphometric analysis. Bioinformatics, 38:2954–2955. https://doi.org/10.1093/bioinformatics/btac173

Speyer, S.E. 1985. Moulting in phacopid trilobites. Transactions of the Royal Society of Edinburgh, 76:239–253. https://doi.org/10.1017/S0263593300010476

Stubblefield, C.J. 1959. Evolution in trilobites. Quarterly Journal of the Geological Society, 115:145–162. https://doi.org/10.1144/GSL.JGS.1959.115.01.08

Teigler, D.J. and Towe, K.M. 1975. Microstructure and composition of the trilobite exoskeleton. Fossils and Strata, 4:137–149.

Vevea, D. and Hall, K.D. 1984. The effects of water temperature on molting and egg production following eyestalk ablation in two species of crayfish, *Orconectes rusticus* and *Orconectes propinquus*. Bios, 55:135–143.

Wang, Y., Esteve, J., Yang, X., Yu, R., and Wang, D. 2023. First confident evidence of moulting in eodiscid trilobites from the Cambrian Stage 3 of South China. Geological Magazine, 160:1441–1445. https://doi.org/10.1017/S0016756823000584

Wang, Y., Peng, J., Wang, D., Zhang, H., Luo, X., Shao, Y., Sun, Q., Ling, C., and Wang, Q. 2021. Ontogenetic moulting behavior of the Cambrian oryctocephalid trilobite *Arthricocephalites xinzhaiheensis*. PeerJ, 9:e12217. https://doi.org/10.7717/peerj.12217

Webster, M. 2007. A Cambrian peak in morphological variation within trilobite species. Science, 317:499–502. https://doi.org/10.1126/science.1142964

Westergård, A.H. 1936. *Paradoxides œlandicus* Beds of Öland. Sveriges Geologiska Undersökning, Avhand-lingar och uppsatser, Series C, 394, 66 pp.

Westrop, S.R. and Adrain, J.M. 1998. Trilobite alpha diversity and the reorganization of Ordovician benthic marine communities. Paleobiology, 24:1–16. https://doi.org/10.1017/S009483730001993X

Whittington, H.B. 1990. Articulation and exuviation in Cambrian trilobites. Philosophical Transactions of the Royal Society of London Series B: Biological Sciences, 329:27–46. https://doi.org/10.1098/rstb.1990.0147

Whittington, H.B., Chatterton, B.D.E, Speyer, S.E., Fortey, R.A., Owens, R.M., Chang, W.T., Dean, W.T., Jell, P.A., Laurie, J.R., Palmer, A.R., Repina, L.N., Rushton, A.W.A., Shergold, J.H., Clarkson, E.N.K., Wilmot, N.V., and Kelly, S.R.A. 1997. Treatise on Invertebrate Paleontology, Part O: Trilobita, revised. Geological society of America and University of Kansas, Boulder, Colorado.

Wickham, H. 2016. ggplot2: Elegant Graphics for Data Analysis. Springer-Verlag, New York. https://cran.r-project.org/web/packages/ggplot2. https://ggplot2.tidyverse.org [R version 4.1.2].

Wickham, H., Averick, M., Bryan, J.,Chang, W., McGowan, L. D., François, R., Grolemund, G. Hayes, A., Henry, L., Hester, J., Kuhn, M., Pedersen, T.L., Miller, E., Bache, S.M., Muller, K., Ooms, J., Robinson, D., Seidel, D.P., Spinu, V., Takahashi, K., Vaughan, D., Wilke, C., Woo, K., and Yutani, H. 2019. Welcome to the Tidyverse. Journal of Open Source Software, 4:1686. https://doi.org/10.21105/joss.01686 [Version 1.3.1].

Yang, J., Ortega-Hernández, J., Drage, H.B., Du, K.-S., and Zhang, X.-G. 2019. Ecdysis in a stem-group euarthropod from the early Cambrian of China. Scientific Reports, 9:5709. https://doi.org/10.1038/s41598-019-41911-w

Zenker, J.C. 1833. Beiträge zur Naturgesichte der Urwelt. Organische Reste (Petrefacten) aus der Altenbruger BraunkohlenFormation, dem Blankenburger Quadersandstein, Jenaischen bunten Sandstein und Böhmischen Uebergangsgebirge. Friedrich Mauke, Jena, 67.

Zong, R. 2020. Coupled exuviae of the Ordovician *Ovalocephalus* (Pliomeridae, Trilobita) in South China and its behavioral implications. PeerJ, 8:e10166. https://doi.org/10.7717/peerj.10166

Zong, R. and Gong, Y. 2022. Allopatric molting of Devonian trilobites. Scientific Reports, 12:13851. https://doi.org/10.1038/s41598-022-18146-3

APPENDIX 1.

All raw data used for the analyses presented here are made freely available with this paper (Drage2023_PE_Supplementarydata.xlsx) and are hosted on the Open Science Framework within the author's project 'The evolution of moulting in Euarthropoda' [https://osf.io/bdx8m/].